CONCRETE RESEARCH LETTERS

www.crl.issres.net Vol. 4 (1) – March 2013

Finite Element and Modal Analysis of 3D Jointless Skewed RC Box Girder Bridge

Mahmoud Sayed-Ahmed[c], Khaled Sennah
Department of Civil Engineering, Faculty of Engineering, Architecture & Science
Ryerson University, CANADA

Abstract

The principal modes (normal modes) of vibration for a multi-degree-of-freedom (MDOF) system are used to generalize the 3D coordinates of the two-span skewed, haunched and jointless reinforced concrete box girder bridge, and to define the structural system response for the n-equations of uncoupled motion. Jointless bridges have many advantages over the conventional construction methods. It has long-term benefits in terms of serviceability, durability, construction cost and maintenance. However it has been limited for nonskewed and light-skewed bridges. The results of the finite element (FE) and modal analysis are presented to study the influence of the skew angle of 0-, 15-, 30-, 45-, 60- and 75-degrees on the natural frequency for the entire skewed bridge and the structural response for the superstructure covering moment, torsion, shear, axial load, deformation at the start and end abutment connection for the entire bridge section subjected to simulated two-perpendicular earthquake forces.

Keywords: Skewed Box Girder Bridge; Reinforced Concrete; Dynamics, Modal Analysis, Earthquake.

1. Introduction

The bridge superstructure can be constructed with skew geometrical deck where the need to understand the behaviour of such structure under moving vehicle-structure-interaction (VSI), soil-structure-interaction (SSI) or any dynamic behaviour are needed. *Modal analysis* studies the dynamic properties or "structural characteristics" of a mechanical structure under dynamic excitation for: (1) resonant frequency; (2) mode shapes; and (3) damping. This research studies a 3D finite element model for continuous-two-span jointless skewed bridge subjected to earthquake with seismic load in x- and y-directions. The results obtained from the 3D modelling can be used to provide useful information and understanding for the behaviour of skew bridge showing; modal frequency; diagonal deformation in the

[c] Corresponding Author: Mahmoud Sayed Ahmed
Email: m.sayedahmed@alumni.ryerson.ca Telephone: +883.510.009.086.476 Fax: +20.2.26327563

jointless two-span haunched skewed reinforced concrete (R.C.) box girder bridge; moment about horizontal and vertical axis; shear vertical and horizontal; torsion; and axial forces.

For newly bridge construction, the national bridge authorities in North America are encouraging the removal or avoidance of expansion joints to improve bridge deck durability in which such bridges are called *Integral Abutment and Jointless Bridges* (IAJB). One of the most merits of the IAJB is reduction of corrosion problem involving leaking expansion joints and seals that that permit salt-laden run-off water from the roadway surface to attack the girder ends, bearing, and supporting reinforced concrete substructure. To avoid structural damage, bridge must rigid to the vehicle-structure-interaction, and flexible to accommodate movement caused by soil-structure-interaction, temperature, skew angle and other factors [1]. In the meantime the construction of skewed jointless bridge is limited to skew angle of 0- and 15-degrees. Kim and Laman investigated the long-term behaviour of integral abutment bridge (IAB) and developed numerical modelling that accounts for the irreversible soil-structure-interaction and time-dependent effects of superstructure [2].

Meng and Lui studied the seismic response of a skew reinforced concrete box girder using finite element models. The study demonstrated that the seismic response of the bridge is affected quite by the boundary conditions of the bridge columns and the overall skewness of the bridge [3]. Ashebo et al. conducted a field measurement to evaluate the dynamic loads on an existing skew box girder continuous bridge with truck load. The study found that the influence of skew in both the static and dynamic behaviours of the bridge within the skew angle range of 0- to 30-degrees is very small [4]. Based on the same model Ashebo et al. proposed dynamic load factor (DLF) based on the vehicle-structure-interaction with values less than what is provided by design codes [5]. Yang et al. extracted the vibration frequencies of the supporting bridge from the dynamic response recorded for the test vehicle during its passage over the bridge, which is referred as indirect approach for measuring the bridge frequencies [6]. Later Yang et al. applied some filters to differentiate between the vehicle frequency and bridge frequency [7].

The conventional and existing simply-supported bridges or continuous span bridges ended as simply-supported structure can be converted to semi-continuous deck system and semi-integral bridge abutment either by link slab or extended slab. Lam et al. (2008) monitored the field performance for the flexible link slab system over the piers for bridges in Toronto City [8] in replacement of the previous expansion joints, converting two simply-supported spans bridge to semi-continuous bridge. Furthermore the authority limited the use of the link slab to girder depth to be less than 1.2 m and to skewness of 20-degrees which is the same limitation for regular skew bridge. Bakht (1988) developed a dimensionless characterizing parameters ξ. The study recommended that if $\xi = S\tan\phi/L$ less than 0.05 then the bridge can be analyzed as right bridge, where S, L, ϕ are the girder spacing, bridge span, and angle of skew respectively [9].The combining link slab over the piers and extended slab linked to the abutment affects the dick sliding over the backwall and revising bearings. Fig.1 presents schematic diagram for two spans simply-supported bridges, and for illustration purpose only it shows link slab over the bent-beam, and extended slab connected to the abutment in what is called semi-integral abutment.

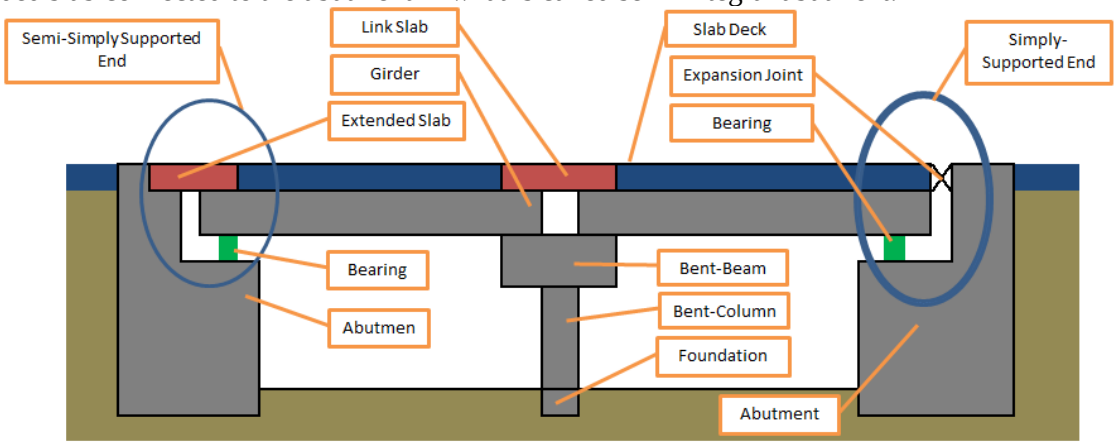

Figure 1: Bridge schematic diagram

This research investigates the response of *skewed jointless bridge deck* subjected to simulated artificial earthquake under its own mass without live load effect. Skew deck is an oblique four-sided parallelogram shape with acute and obtuse angles, where each type of angle is located diagonally: (1) acute-acute diagonal; (2) obtuse-obtuse diagonal. This type of irregular geometry was set to be designed as straight bridges even with skew angle of 15-degrees neglecting the effect of torsion, using method like grillage method or finite differences, and even when such methods are used it becomes difficult to idealize such geometry ending with simplifying the geometry to provide approximate deflection measurement for the slabs neglecting the unseated behaviour and rotational effect.

The 3D-FEM presented the structural response for the rotational behaviour and the diagonal translations in x-, y-, and z-directions for skewed jointless bridge deck under different skew angles of 0-, 15-, 30-, 45-, 60- and 75-degrees. Converting conventional bridge to jointless bridge may be performed by changing the connection types, converting the simply-supported slabs to continuous slab by replacing the expansion joints with link-slab made of engineered cementitious composite (ECC) [10, 11] materials and/or connect the deck to the bent-column and abutment. Designer and researchers for these types of new connections usually provide testing for their products only in z-direction for the link-slab, and only in x- and y-direction for the bearing and abutment connections. This paper is trying to point out the importance to consider the 3D dimensional effect rather than considering one dimensional effect for testing link-slabs, and 2D dimensional effect for testing the bearing connections.

2. Research Significance

Numerical modelling for prestressed concrete box-girder bridge with integrated bent-column is modelled in SAP2000 to investigate the skewness effect, and clarify the consequences if skewed bridge is idealized as if it is straight bridge for live load using load control technique (LC), as the common practice up to 20-degree. But if the same bridge was subjected to lateral loading due to earthquake which is displacement control (DC) technique, the response will differ.

3. Numerical Model

3.1. Modal Participation Factor

The general matrix formulation of the equation of motion for an undamped multi-degree-of-freedom (MDOF) system subjected to external excitation is given by EQ. 1, where [k] and [m] are the symmetric n X n stiffness and mass matrices, respectively. {x} and $\{\ddot{x}\}$ are the n X 1 displacement and acceleration force vectors (in physical coordinates) respectively, and {F(t)} is the n X 1 external force vector. This coupled equation solved in simultaneously basis through the stiffness matrix and the mass matrix contains off-diagonal terms.

$$[m]\{\ddot{x}\} + [k]\{x\} = \{F(t)\} \quad \text{(EQ.1)}$$

The displacement $\{x(t)\}$ due to forced response for a MDOF system is shown in EQ. 2 [12].

$$\{x(t)\} = \sum_{r=1}^{n} \{\Phi\}_r \Gamma_r R_r(t) \quad \text{(EQ. 2)}$$

Where $\{\Phi\}_r$ is the modal vector for the rth normal mode; Γ_r is referred to as the modal participation factor for the rth mode in [mm]; and $R_r(t)$ is the response ratio corresponding to the rth mode. Thus the dynamic response for the rth mode expressed in principal coordinates as

$$q_r(t) = \Gamma_r R_r(t) \quad \text{(EQ. 3)}$$

Where

$$\Gamma_r = \frac{P_r}{K_r} = \frac{\{\Phi\}_r^T\{F_o\}}{\{\Phi\}_r^T\{k\}\{\Phi\}_r} = \frac{\{\Phi\}_r^T\{F_o\}}{(\omega_r)^2\{\Phi\}_r^T\{m\}\{\Phi\}_r} \quad \text{(EQ. 4)}$$

Where $q_r(t)$ is the time-history response; $\{\Phi\}_r^T$ is the transpose of $\{\Phi\}_r$; ω_r is the undamped natural circular frequency for the rth normal mode; $\{k\}$ is the stiffness matrix; $\{m\}$ is mass matrix; and $\{F_o\}$ is amplitude vector for external harmonic force. Response spectrum analysis; in such instances a response spectrum analysis is used. The maximum modal response for the rth mode of a MDOF system to a specified input, expressed in physical coordination

$$(\{x\}_r)_{max} = \sum_{r=1}^{n} | \{\Phi\}_r \Gamma_r (DMF)_r | \quad \text{(EQ. 5)}$$

Where $(\{x\}_r)_{max}$ is the maximum displacement response for the rth mode in [**mm**]; $\{\Phi\}_r$ is modal vector for the rth mode; Γ_r is the modal participation factor for the rth mode; $(DMF)_r$ is the dynamic magnification factor for the rth mode determined from the appropriate response spectrum. The statistical combination of the maximum modal responses have is known as the squares root of the sum of the squares (SRSS) which is the popular method for combining modal maxima [12].

$$\{x\}_{max} = [\sum_{r=1}^{n} (\{\Phi\}_r \Gamma_r (DMF)_r)^2]^{\frac{1}{2}} \quad \text{(EQ. 6)}$$

The result from this displacement control method is applied to EQ.1 after that.

4. Parametric Study

4.1. Reinforced Concrete Box Girder Bridge

The numerical study investigates the axial force-combined interaction for two-span concrete box girder as shown in Figs 2 and 3. The bridge superstructure is shown in Fig. 4 comes with the following specifications and dimensions; f_c'= 40 MPa, four girders, total width of the deck is 10.9728 m, and the deck depth is 1.524 m. The top and bottom slab thickness t_1 = 0.3048 m, t_2 = 0.2032 m respectively. The girders thickness is 0.3048 m each. The horizontal fillet dimensions are 0.1524 m and 0.4572 m for two sets respectively. The first set contains f_3 and f_6. The second set contains f_1, f_2, f_4, f_5, f_7, f_8. The vertical fillet f_1 through f_8 all equals to 0.1524 m. The overhang dimensions L_1, L_2 equal to 0.9144 m, and its outer thickness t_5, and t_6 equals to 0.2032 m. The bridge has a solid diaphragm with thickness of 0.3048 m.

The bridge substructure has two main substructure elements; the abutment, and the integrated bent. The abutment located the two edges of the bridge deck has a length of 9.144 m, depth of 2.4384 m, and width of 1.2192 m. Foundation springs used for abutment was assigned as fixed for all degree of freedom (DOF) and directions. The integrated bent has two main elements the bentcap (beam) and the bent-column. The cap beam has a length of 9.144 m, depth of 3.048 m and width of 1.524 m. The bent column has a diameter of 1.524 m. This bentcap has 3 columns located at 0.762 m, 4.572 m, and 8.382 m from the edge of the cap length, the columns height is 7.3152 m with fixed base support. Table 1 shows the properties of the link elements used to connect the studied model.

This continuous concrete box girder bridge has a parametric thickness variation, as its thickness at the two edges equal to 1.524 m and at the bentcap equals to 3.048 m. The deck length from span to the bentcap is 33.528 m. The deck is post-tensioned by prestress tendons, jacked from the start point. The tendon's material property marked as A416Gr270 with area of $6.452 \times 10^{-3} m^2$.

TABLE 1: LINK/SUPPORT PROPERTIES

Link Property	Link Type	Directions	Line Spring	Remarks
BBRG1-2	Linear	U1 and U2	1000 kN/mm	Girder-Abutment connection
BFIXSS-2	Linear	U1, U2, U3 R1, R2, R3	1000 kN/mm	From deck and top of the girder to the bent-beam (0 to -2946.4 mm)
Fixed-2	Linear	U1, U2, U3 R1, R2, R3	1000 kN/mm	From the centerline of the girder to bent-beam (0 to -1524 mm)
Foundation Spring	Linear	U1, U2, U3 R1, R2, R3		Foundation of Bent-columns are restraints in all directions

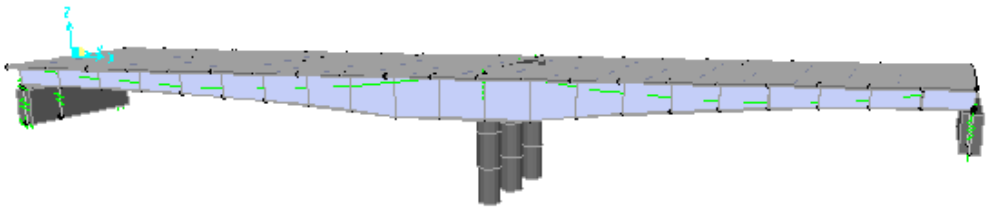

Figure 2: Two-span haunched R. C. box girder bridge

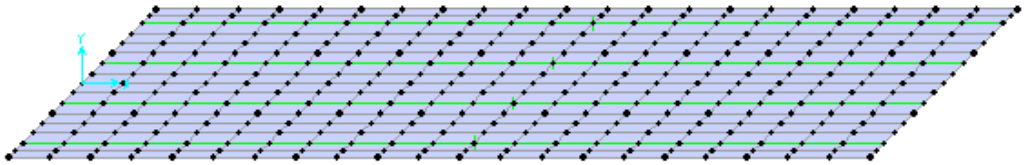

Figure 3: The 45 degree skewed slab deck

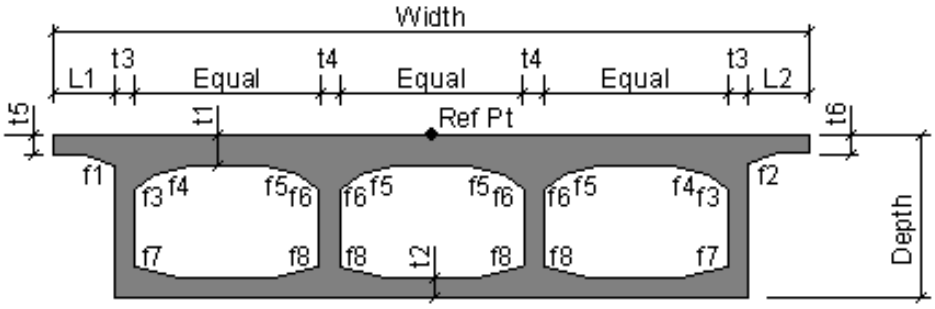

Figure 4: Vertical R. C. box girder bridge section (extracted from sap2000)

Load Cases

SAP2000 version 14 was used to calculate the effect of the earthquake load and effects, based on the Time History function generated from Los Angeles Century City (LACC) at 0- and 90-degrees to the bridge structure for 3000 data within 60 seconds as shown in Fig. 5. The load case type was selected for Modal, type of modes to be Ritz vectors, number of modes is 30. The load type was assigned dead for load pattern, UX & UY for Accel and All for link, with 99% of target dynamic participation ratio. SAP2000 has the default design combo option for "Add Code-Generated User Load Combination" that generated different load combination for bridge design according to the AASHTO [13]. However the presented analysis was limited to study the combinational effect for the mass $[m]$ of the bridge, the vibrational modal modes $\{\Phi\}_r$ and the different skew angles for the bridge deck.

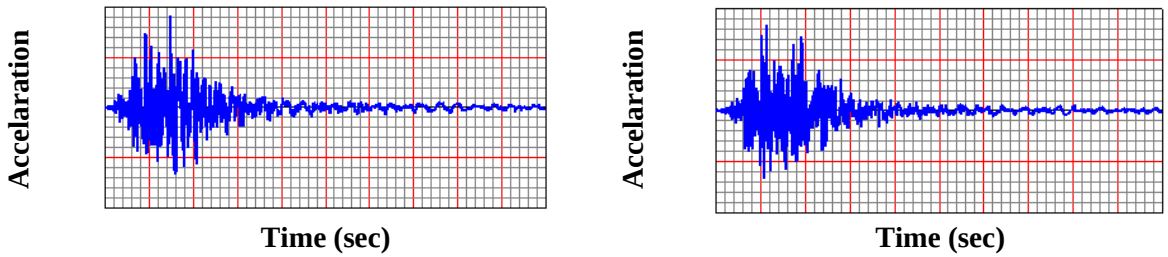

(a) LACC 0-degree (b) LACC 90-degree

Figure 5: Time History

5. Results

Table 2 shows that the modal frequency increases with the increase of the skew angle from 0- to 60-degrees and then started to decrease when the skew angle increases to 75 degrees for the any single modal mode. The frequency also increases with the increase of the modal mode. It was notices the modal frequencies are almost identical for the skew angles of 15- and 75-degrees. Fig. 6 shows the 3D deformation under the modal mode with respect to the skew angle of the superstructure.

Table 3 show the diagonal deformation in the jointless two-span haunched skewed R.C. box girder bridge for the both edges at the acute and obtuse angles. At zero skew the diagonal deformations are constant all over the 5 different modal modes, with the increase of the skew angle of 15-degrees; the diagonal deformation was almost the same in the first mode and then started to change with higher modes. The irregular diagonal deformations lead to in-plane rotation of the bridge deck. It is noticed that the initial diagonal deformation values obtained from the first mode increases with the increase of the skew angle.

In terms of moment, as shown in Figs. 7 and 8, skew deck has two values of moment in the horizontal and vertical directions. The higher moment values about the horizontal axis obtained from the zero skew decks and decreases with the increase of the skew angle. For moment about vertical axis the lowest value is recorded for the zero skew, and the highest value go for the 45 degrees, while 15 and 75 degrees recorded a close value to the zero skew deck. Skewed bridge has shear values in two components the horizontal and vertical direction as shown in Figs. 9 and 10. The vertical shear values for the skew deck shows the highest value for the zero skew deck, where vertical shear decreases with the increase of the skew angle. In contradict the horizontal shear value is zero for zero skewed deck and increases of skew angle up to 45 degrees afterward shear values start to decrease again, even values of 15 and 75 degrees are in good agreement together. Fig. 11 shows that the torsion values increases with the increase of skew angle up to 45 degree and then decreases again. The axial force values increases with the increase of the skew angle, and due to the external dynamic excitation; Fig. 12 shows that the bent columns are the most critical structural elements to resist such loads.

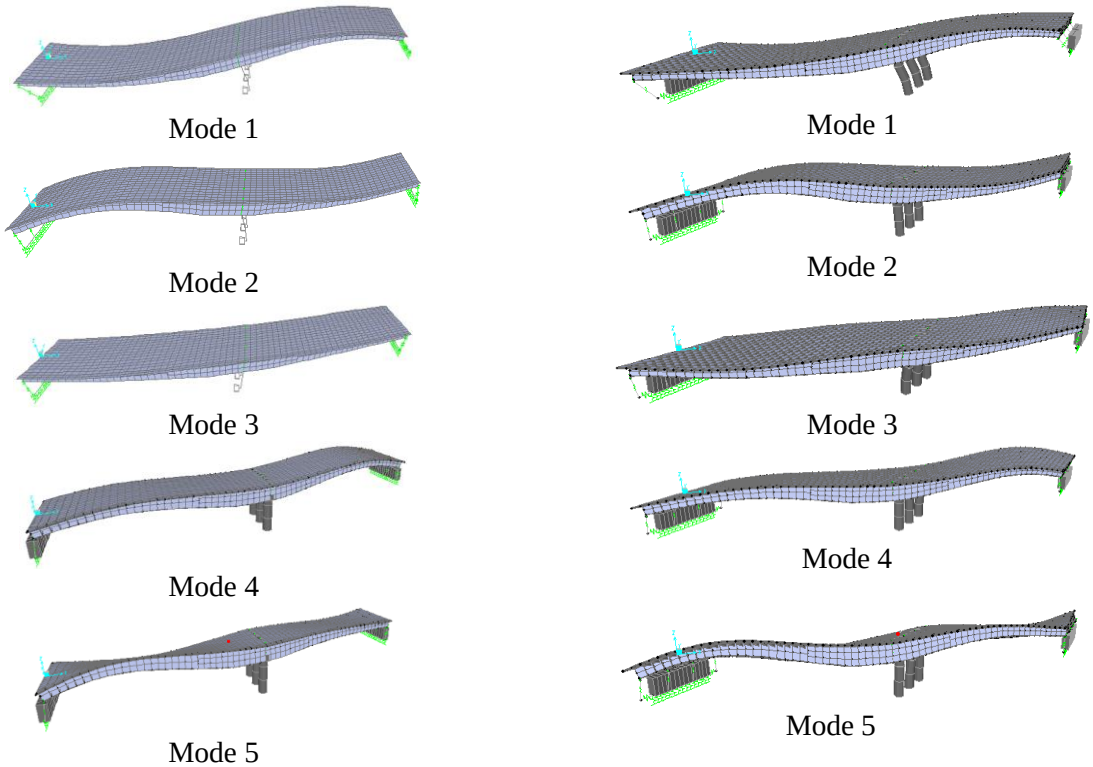

(a) Skew of 15-degree (b) Skew of 45-degree

Figure 6: Deformation modes for skewed bridge of 15- and 45-degrees

TABLE 2: INFLUENCE OF SKEW ANGLE ON NATURAL FREQUENCY

Skew angle (^{o})	Modal frequency (Hz)				
	Mode 1	Mode 2	Mode 3	Mode 4	Mode 5
0	2.77016	4.394252	5.397819	5.969793	11.46263
15	2.790101	4.375985	5.398985	6.007088	11.14827
30	2.931004	4.586735	5.455835	6.154982	10.40799
45	3.123731	5.065856	5.525167	6.471654	9.567547
60	3.320274	5.555247	6.11546	7.04821	9.041591
75	2.790101	4.375985	5.398985	6.007088	11.14827

TABLE 3: DIAGONAL DEFORMATION IN THE JOINTLESS TWO-SPAN HAUNCHED SKEWED R.C. BOX GIRDER BRIDGE

Skew angle (^{o})	Mode	Diagonal deformation into x, y, z (mm)			
		Left Side		Right Side	
		Acute angle	Obtuse angle	Acute angle	Obtuse angle
0-	1	-23.8, 0.0, -0.1	-23.8, 0.0, -0.1	-24.1, 0.0, 0.1	-24.1, 0.0, 0.1
	2	-20.1, 0.0, 0.3	-20.1, 0.0, 0.3	-19, 0.0, -0.2	-19, 0.0, -0.2
	3	10.6, -1.9, 0.4	10.6, -1.9, 0.4	-10, -1.7, 0.4	-10, -1.7, -0.4
	4	0.5, 0.0, 0.4	0.5, 0.0, 0.4	5.1, 0.0, 0.6	5.1, 0.0, 0.6
	5	6.5, -7.8, -4.9	6.5, -7.8, 4.9	10.4, 4.9, -0.6	10.4, 4.9, 0.6
15-	1	-24.4, -1.1, 0.0	-25.6, -0.8, -0.4	-24.7, -1, 0.0	-25.7, -0.6, 0.4
	2	-19.4, 2.4, 0.1	-18, 2, 0.8	-18.2, 1.5, -0.1	-17, 1.1, -0.5
	3	-10.7, 0.6, -0.1	10, -5.1, 0.7	-10.4, 0.9, 0.0	9.3, -4.5, -0.7
	4	-0.3, 2.3, 0.2	0.9, 2.1, 0.5	5.0, -3.4, 0.3	4.6, -3.4, 0.9
	5	-2.8, 6.3, 2.8	1.0, 7.0, -6.8	-5.6, 2.0, -1.0	4.7, -0.4, 2.1
30-	1	-25.7, -2.1, 0.0	-27.5, -0.9, -0.8	-25.9, -1.9, 0.0	-27.7, -0.7, 0.8
	2	-17.6, 5.6, 0.0	-14.8, 3.8, 1.5	-16.2, 3.3, 0.0	-13.9, 1.8, -1.1
	3	-10.2, 2.3, 0.4	9.0, -9, 0.9	-10.1, 3.1, -0.4	8.3, -7.7, -1.0
	4	-0.7, 5, 0.1	1.5, 3.9, 0.5	5.3, -7.5, 0.0	4.1, -6.8, 1.4
	5	-6.2, 10.3, 0.6	4.5, 6.9, -7.9	-5.1, 6.7, -0.4	4.0, 3.0, 4.4
45-	1	-27.9, -2.3, -0.1	-29.5, -0.4, -1.2	-27.9, -2.1, 0.1	-29.6, -0.1, 1.2
	2	-13.8, 10.4, 0.1	-9.9, 6.0, 3.1	-12.0, 5.4, -0.1	-9.2, 2.1, -2.2
	3	-9.1, 3.1, 0.1	7.2, -13.5, 1.7	-9.2, 4.2, -0.9	6.9, -12.0, -1.8
	4	-0.7, 8.1, -0.1	2.0, 6.0, 0.3	6.0, -13.4, -0.2	2.9, -10.3, 2.3
	5	-7.3, 16.1, -0.5	7, 6.1, -10.6	-5.9, 12.3, 0.3	5.6, 3.8, 7.4
60-	1	-29.7, -1.6, -0.1	-30.5, 0.2, -1.6	-29.6, -1.5, 0.1	-30.5, 0.4, 1.6
	2	-0.5, 9.0, -1.2	-7.3, 20.6, -2.5	0.8, 3.2, 1.1	-7.3, 16.8, 3.2
	3	-11.8, 18.7, 1.1	0.3, -27.5, 7.3	-8.9, 6.3, -1.1	0.1, -9.9, -5.7
	4	0.5, 10, -0.4	1.8, 9.0, -1.7	8.2, -25.6, 0.0	-0.2, -11.7, 3.1
	5	-6.6, 21.7, -0.2	9.5, 1.2, -18.3	-5.2, 16.3, 0.0	7.6, -0.3, 13.6
75-	1	-30.2, -1.4, -0.3	-30.0, -0.6, -0.7	-30.0, -1.3, 0.4	-30.0, -0.5, 0.4
	2	-6.0, 25.0, 1.6	-2.6, 17.5, -12.7	-4.9, 18.4, -1.0	-3.1, 16.0, 12.8
	3	-4.2, 27.2, 2.9	2.9, 2.6, 1.3	5.4, -35.2, 3.4	-1.9, -10.4, -4.6
	4	5.9, -17.9, -5.8	-7.2, 33.0, -9.3	6.8, -23.2, 6.6	-7.6, 32.3, 8.3
	5	-13.6, 84.5, 25.4	5.8, 3.8, -33.8	2.8, -11.7, 2.6	-0.8, -3.5, -0.5

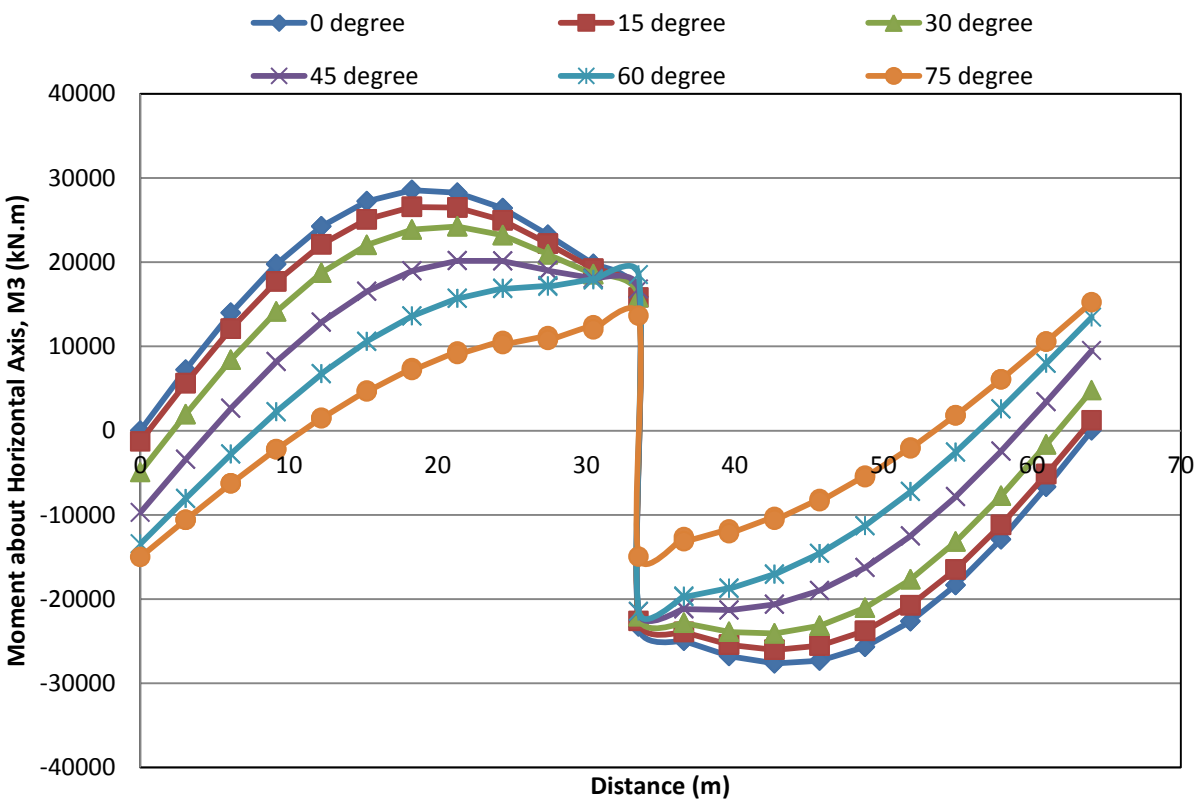

Figure 7: Moment about horizontal axis

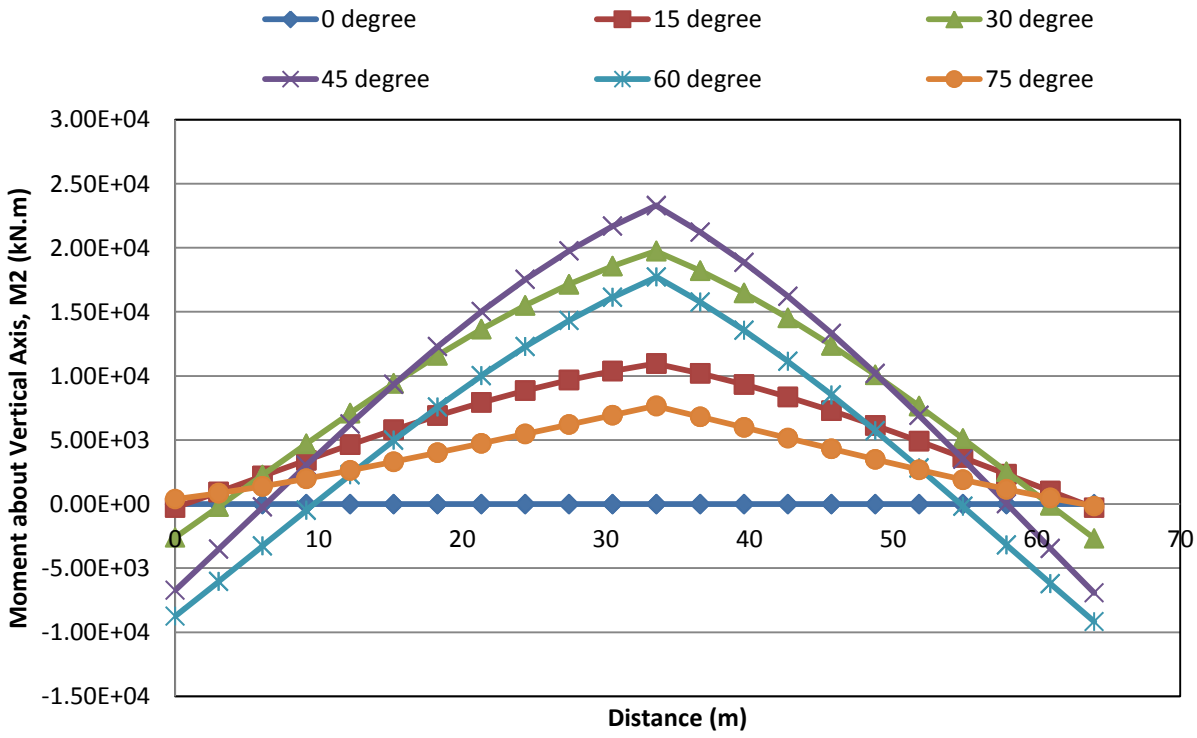

Figure 8: Moment about vertical axis

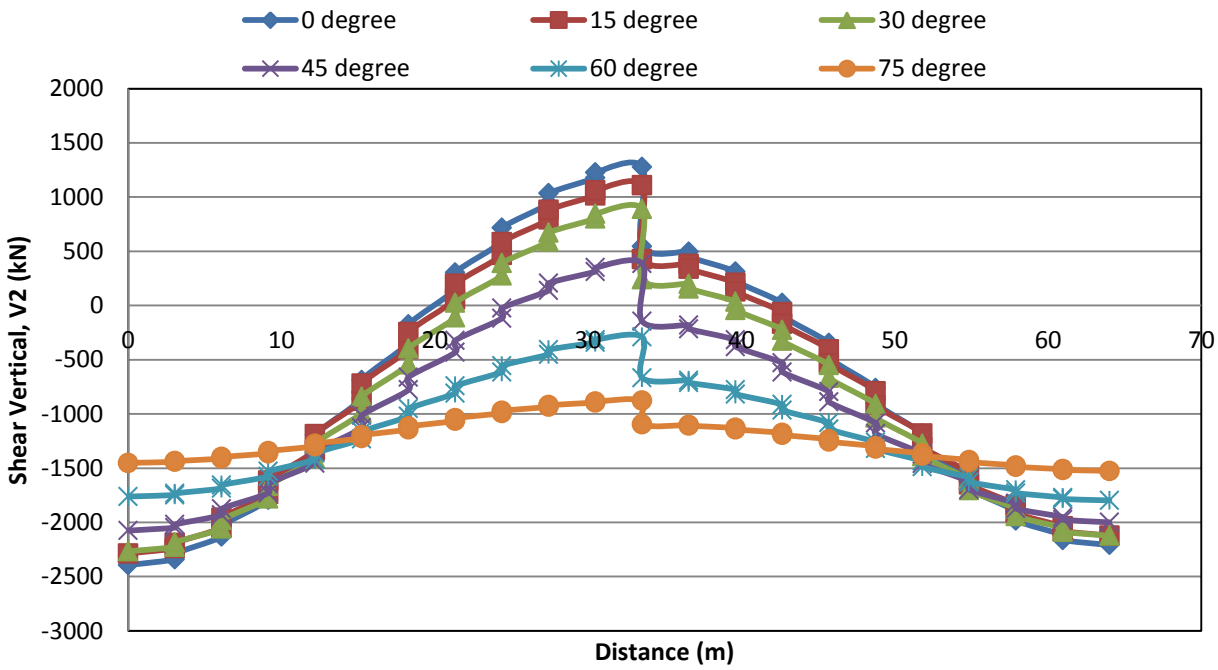

Figure 9: Shear vertical

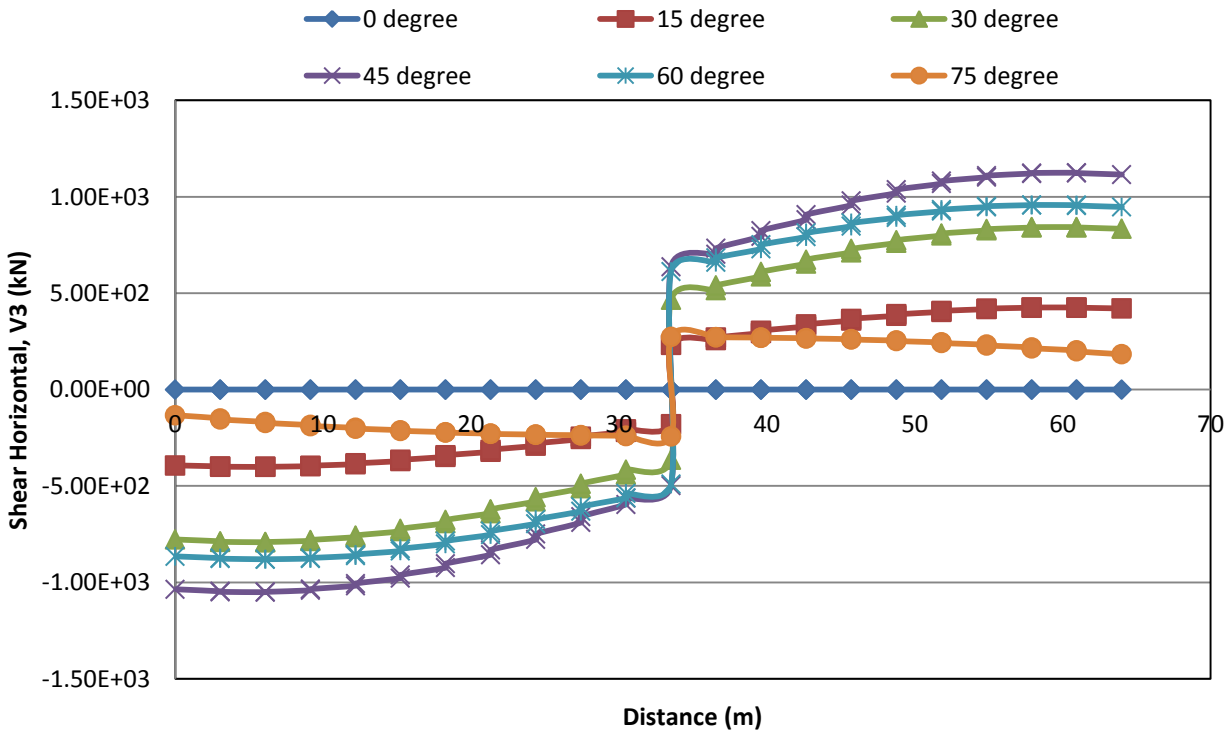

Figure 10: Shear horizontal

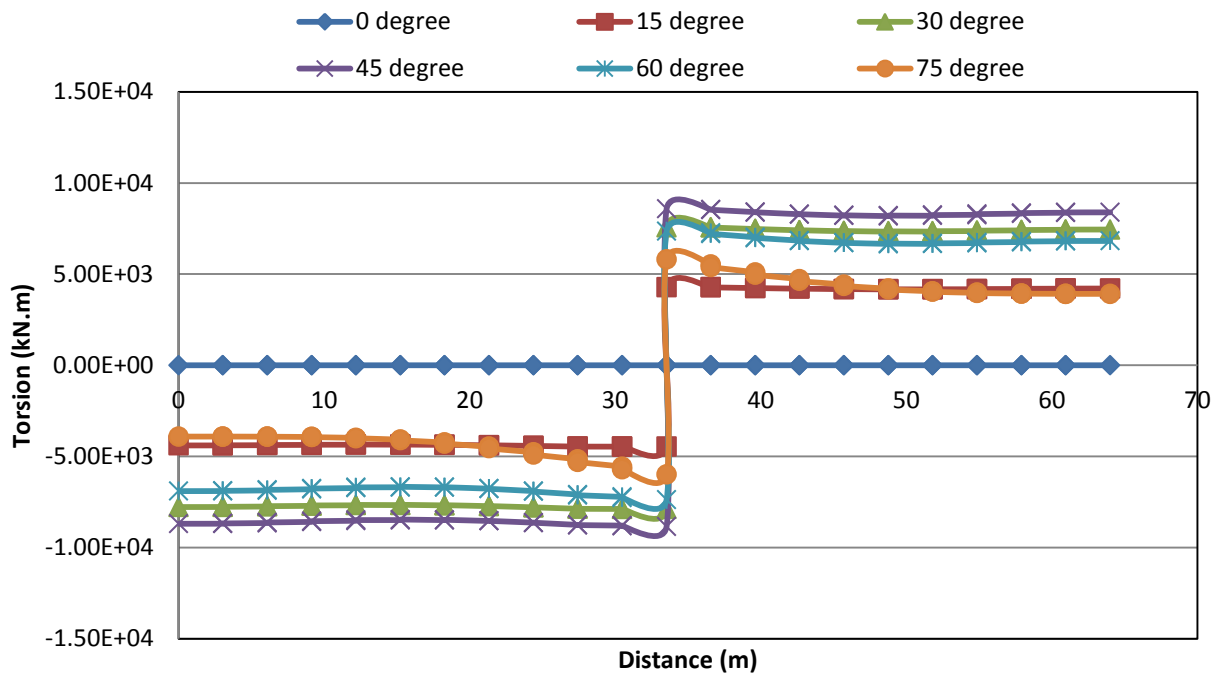

Figure 11: Torsion

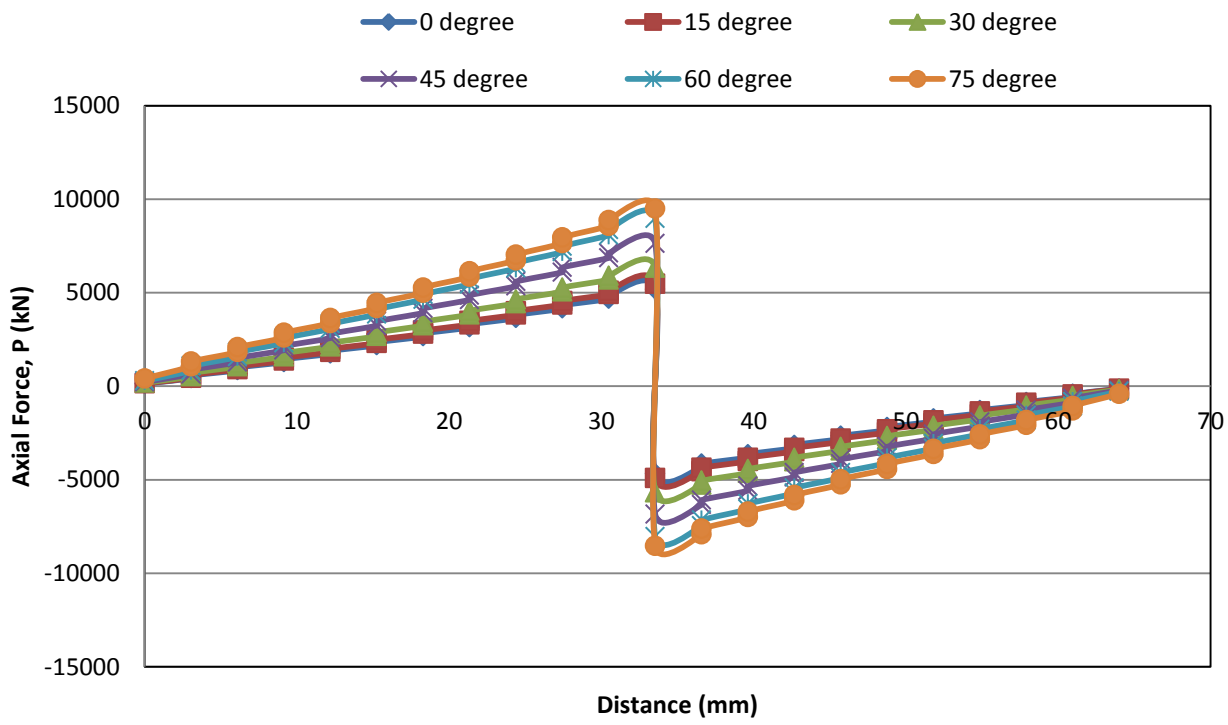

Figure 12: Axial force

General behaviour indicates that vertical shear (perpendicular to direction of the travelling lane) is quite small. The horizontal shear (parallel to direction of the travelling lane) should be considered in combined with torsion generated from the skew alignment of the girders. The shear-torsion effect increases with the increase of the skew angle from 0- to 45- degree then decreases as it shown in Figs. 10 and 11.

6. Conclusions

This study provides 3-dimensional structural response of jointless bridge deck subjected to simulated earthquake. SAP2000 generates nonlinear modal response of multi-degree of freedom (MDOF) structure. The 3D finite element model revealed the following:

Modal analysis reveals that skewed bridge deck will not deform constantly through the deck's diagonal corners, leading to 3D in-plane and out-plane rotation and translation that could dramatically increase with the addition of different types of loading.

The easily implemented non-destructive and numerical techniques used to simulate the seismic and modal behaviour with different skew angles reveals that moment values increases with the increase of skew angle up to 45-degree and decreases afterward. The maximum vertical shear is found to be at the 0-angle, while the maximum horizontal shear found to be at the 45-degrees. The skewness creates torsion and its maximum values found at the 45-degrees. For continuous slab and in seismic period the most critical structural elements will be the substructure elements.

In converting the conventional simply-supported bridge to jointless semi-continuous bridge, designer should consider the 3D effect for all connections.

7. Recommendations

Investigate the effect of different boundary conditions used in defining the finite element for skewed reinforced concrete structure which is highly sensitive to its boundary conditions; (1) located at the abutment representing the soil-structure-interaction; (2) at connection between skewed precast elements; and (3) material nonlinearity considering the glass fibre reinforced polymers (GFRP). Conduct parametric study for different span/width ratios, span/thickness ratio with different skew angles.

References

[1] J. Burk and P. Martin, *An Introduction to the Design and Construction of Integral Bridges, Workshop on Integral Bridges, Nov 13-15,* West Virginai: FHWA West Virginai and West Virginia University, 1996.

[2] W. Kim and J. A. Laman, "Numerical analysis method for long-term behavior of integral abutment bridges," *Engineering Structures,* vol. 32, no. 8, pp. 2247-2257, 2010.

[3] J. Y. Meng and E. M. Lui, "Seismic analysis and assessment of a skew highway bridge," *Engineering Structures,* vol. 22, no. 11, pp. 1433-1452, 2000.

[4] D. B. Ashebo, T. H. Chan and L. Yu, "Evaluation of dynamic loads on a skew box girder continuous bridge Part I: Field test and modal analysis," *Engineering Structures,* vol. 29, no. 6, pp. 1052-1063, 2007.

[5] D. B. Ashebo, T. H. Chan and L. Yu, "Evaluation of dynamic loads on a skew box girder continuous bridge Part II: Parametric study and dynamic load factor," *Engineering Structure,* vol. 29, no. 6, pp. 1064-1073, 2007.

[6] Y. B. Yang, C. W. Lin and J. D. Yau, "Extracting bridge frequencies from the dynamic response of a passing vehicle," *Journal of Sound Vibration,* vol. 272, pp. 471-93, 2004.

[7] Y. B. Yang, K. C. Chang and Y. C. Li, "Filtering techniques for extracting bridge frequencies from a test vehicle moving over the bridge," *Engineering Structures,* vol. 48, pp. 353-362, 2013.

[8] C. Lam, D. Lai, J. Au, L. Lim, W. Young and B. Tharmabala, "Development of Concrete Link Slabs to Eliminate Bridge Expansion Joints Over Piers," in *Annual Conference of the Transportation Association of Canada*, Toronto, 2008.

[9] B. Bakht, "Analysis of Some Skew Bridges as Right Bridges," *Journal of Structural Engineering,* vol. 114, no. 10, pp. 2307-2322, 1988.

[10] S. Qian, V. C. Li, H. Zhang and G. A. Keoleian, "Durable and sustainable overlay with ECC," in *9th International Conference on Concrete Pavements*, San Francisco, 2008.

[11] S. Qian, M. D. Lepech, Y. Y. Kim and V. C. Li, "Introduction of Transition Zone Design for Bridge Deck Link Slabs Using Ductile Concrete," *ACI Structural Journal,* vol. 106, no. 1, pp. 96-105, 2009.

[12] J. W. Tedesco, W. G. McDougal and C. Allen, Structural dynamics: theory and applications, 1999.

[13] AASHTO, *AASHTO LRFD bridge design specifications, 5th Edition*, Washington, DC: American Association of State Highway and Transportation Officials, 2010.

[14] Canadian Standard Association, Canadian Highway Bridge Design Code, CAN/CSA-S6-06, Ottawa: Canadian Standard Association, 2006.